Headgroup Hydration and Mobility of DOTAP/DOPC Bilayers: A Fluorescence Solvent Relaxation Study

Piotr Jurkiewicz,[†,‡,§] Agnieszka Olżyńska,[†,§] Marek Langner,[‡] and Martin Hof*[,†]

J. Heyrovský Institute of Physical Chemistry, Academy of Sciences of the Czech Republic, Dolejškova 3, CZ-18223 Prague 8, Czech Republic and Institute of Physics, Wrocław University of Technology, Wybrzeże Wyspiańskiego 27, 50-370 Wrocław, Poland

Received June 2, 2006. In Final Form: August 14, 2006

The biophysical properties of liposome surfaces are critical for interactions between lipid aggregates and macromolecules. Liposomes formed from cationic lipids, commonly used to deliver genes into cells in vitro and in vivo, are an example of such a system. We apply the fluorescence solvent relaxation technique to study the structure and dynamics of fully hydrated liquid crystalline lipid bilayers composed of mixtures of cationic dioleoyltrimethylammoniumpropane (DOTAP) and neutral dioleoylphosphatidylcholine (DOPC). Using three different naphthalene derivatives as fluorescent dyes (Patman, Laurdan and Prodan) allowed different parts of the headgroup region to be probed. Wavelength-dependent parallax quenching measurements resulted in the precise determination of Laurdan and Patman locations within the DOPC bilayer. Acrylamide quenching experiments were used to examine DOTAP-induced dye relocalization. The nonmonotonic dependence of dipolar relaxation kinetics (occurring exclusively on the nanosecond time scale) on DOTAP content in the membrane was found to exhibit a maximum mean solvent relaxation time at 30 mol % of DOTAP. Up to 30 mol %, addition of DOTAP does not influence the amount of bound water at the level of the sn_1 carbonyls, but leads to an increased packing of phospholipid headgroups. Above this concentration, elevated lipid bilayer water penetration was observed.

Introduction

Gene therapy offers extraordinary long-term potential for the treatment of human diseases, including inherited and acquired disorders, cancer, and AIDS. The main problems in this field include the shortcomings of gene transfer vectors and an inadequate understanding of the biological interaction of these vectors with the host. In particular, since the introduction of liposomal transfection agents,[1] low efficiency was a limiting factor for using these otherwise safe and reliable gene carriers. To enhance and maintain a high level of tissue-specific and regulated expression of transferred genes and also to improve drug stability and shelf life, greater focus is required on the basic aspects of gene transfer.

The association of nucleic acids with lipid compounds has been carried out with the assumption of two opposite charges—a negative one on nucleic acids and a positive one on the lipid surface—leading to formation of a stable complex (lipoplex). Such an effect is indeed experimentally observed.[2−5] Reducing the process to simple electrostatics, however, results in poor control over compound association and an ill-defined structure of the lipoplex. There are likely to be other factors besides electrostatics that influence the association process. The lipid surface is commonly altered by changing lipid composition, adding a "helper lipid", modifying the positively charged lipid compound,[2,6,7] or grafting the surface with a polymer.[8−10] No quantitative measures of such alterations exist, and the approach is therefore usually reduced to trial and error. Cationic liposomes share common properties with biological and model lipid membranes, and both can be studied using similar experimental techniques.

While many functions have been assigned to membrane proteins,[11] the lipid bilayer has for a long time been perceived almost exclusively as a passive structural element, despite growing knowledge of the involvement of lipids in a variety of cellular processes.[12−15] Following that perception, drastically simplified models are often used for lipid bilayers when their functions are discussed.[16,17] Such a paradigm results in a myriad of studies that aim almost exclusively at correlating lipid bilayer properties with the state of the membrane hydrocarbon chain region, disregarding its real complexity.[18] This oversimplification has been seriously challenged by the discovery of lipid domains in model lipid bilayers and rafts in biological membranes.[19−25]

* To whom correspondence should be addressed. E-mail: martin.hof@jh-inst.cas.cz.

† Academy of Sciences of the Czech Republic.

‡ Wrocław University of Technology.

§ Contributed equally.

(1) Felgner, P. L.; Gadek, T. R.; Holm, M.; Roman, R.; Chan, H. W.; Wenz, M.; Northrop, J. P.; Ringold, G. M.; Danielsen, M. *Proc. Natl. Acad. Sci. U.S.A.* **1987**, *84*, 7413−7417.

(2) Hui, S. W.; Langner, M.; Zhao, Y. L.; Ross, P.; Hurley, E.; Chan, K. *Biophys. J.* **1996**, *71*, 590−599.

(3) Kral, T.; Benda, A.; Hof, M.; Langner, M. In *Review of Fluorescence*; Geddes, C. D., Lakowicz, J. R., Eds.; Springer: New York, 2005; Vol. 2, p 109.

(4) Kral, T.; Hof, M.; Jurkiewicz, P.; Langner, M. *Cell. Mol. Biol. Lett.* **2002**, *7*, 203−211.

(5) Radler, J. O.; Koltover, I.; Salditt, T.; Safinya, C. R. *Science* **1997**, *275*, 810−814.

(6) Byk, G.; Sato, J.; Mattler, C.; Frederic, M.; Scherman, D. *Biotechnol. Bioeng.* **1998**, *61*, 81−87.

(7) Byk, G.; Scherman, D. *Exp. Opin. Ther. Patents* **1998**, *8*, 1125−1141.

(8) Hong, K. L.; Zheng, W. W.; Baker, A.; Papahadjopoulos, D. *FEBS Lett.* **1997**, *400*, 233−237.

(9) Martin-Herranz, A.; Ahmad, A.; Evans, H. M.; Ewert, K.; Schulze, U.; Safinya, C. R. *Biophys. J.* **2004**, *86*, 1160−1168.

(10) Borowik, T.; Widerak, K.; Ugorski, M.; Langer, M. *J. Liposome Res.* **2005**, *15*, 199−213.

(11) le-Coutre, J.; Kaback, H. R. *Biopolymers* **2000**, *55*, 297−307.

(12) Luguain, C.; Sciorra, V. A.; Morris, A. J. *Trends Biol. Sci.* **2003**, *28*, 377−383.

(13) English, D.; Welch, Z.; Kovala, A. T.; Harvey, K.; Volpert, O. V.; Brindley, D. N.; Garcia, J. G. N. *FASEB J.* **2000**, *14*, 2255−2265.

(14) Cooke, F. T. *Arch. Biochem. Biophys.* **2002**, *407*, 143−151.

(15) Baird, B.; Shets, E. D.; Holowka, D. *Biophys. Chem.* **1999**, *82*, 109−119.

(16) Cevc, G. *Biochim. Biophys. Acta* **1990**, *1031−3*, 311−382.

(17) Langner, M.; Kubica, K. *Chem. Phys. Lipids* **1999**, *101*, 3−35.

(18) Nagle, J. F.; Tristram-Nagle, S. *Biochim. Biophys. Acta* **2000**, *1469*, 159−195.

10.1021/la061597k CCC: $33.50
Published on Web 09/15/2006

The properties of the lipid bilayer interior are relatively easy to determine experimentally, but the lipid−water interface is little explored.[26,27] This is an unfortunate situation since many processes, ranging from protein folding[28,29] and adsorption[30,31] to the generation of second messengers from lipid precursors,[12,15] take place in this region. It is also the headgroup part of the cationic liposome, which is responsible for interactions with DNA. The region is characterized by large gradients of all relevant physicochemical parameters, providing a complex environment, which can be modified by both alterations of lipid bilayer composition and/or properties of the aqueous phase.[32] This picture is further complicated by the dynamic character of the membrane, the components of which are free to undergo a variety of motions due to thermal agitation as well as macroscale membrane movements that affect the bilayer and adjacent water layers.[18,33,34] The limited availability of experimental data makes validating numerical simulations difficult and suppressed the development of technologies based on supramolecular lipid aggregates.[35,36]

Fluorescence probes are capable of measuring numerous important parameters of lipid membranes, such as local pH, surface-adsorbed compound concentrations, and others.[26,37,38] It is worth noting that the stable location of the reporting molecule within the bilayer is frequently a fundamental concern. Quenching with lipids labeled with free radicals at known positions, followed by parallax analysis, has been successfully applied for this task.[39−41]

Hydration properties of the bilayer (e.g., the amount of water hydrating lipids, the mobility of water molecules, and the mobility of the hydrated lipids) are the main factors responsible for the state of the membrane and the way it interacts with its surroundings. Several experimental methods have been employed to study the hydration of phospholipid membranes (e.g., NMR,[42,43] fluorescence,[44,45] X-ray and neutron diffraction[46,47]). The solvent relaxation technique, based on simple time-resolved fluorescence measurements, can be easily used to measure the amount of water and its mobility in the vicinity of a probe. These quantities are directly related to the value of the total time-dependent Stokes shift and its kinetics, respectively. The uniqueness of this tool, however, lies in its ability to measure liquid crystalline lipid bilayers, which are fully hydrated and thus biologically relevant.[48−50]

In this paper, we show that the solvent relaxation technique can be successfully employed to obtain quantitative data on the molecular level about events occurring within the charged lipid bilayer interface. The nonmonotonic dependence of the properties of fully hydrated liquid crystalline cationic membranes on their cationic lipid content, revealed by recent simulations,[51] seems to be confirmed experimentally. The finding is also in agreement with the phase diagrams obtained for similar cationic lipid systems.[52]

Materials and Methods

Materials. 1,2-dioleoyl-*sn*-glycero-3-phosphocholine (DOPC), 1,2-dioleoyl-3-trimethylammoniumpropane (DOTAP), and 1,2-dioleoyl-*sn*-glycero-3-phospho(Tempo)choline (TEMPO) were obtained from Avanti Polar Lipids, Inc. (Alabaster, AL). All fluorescence probes, namely, 6-hexadecanoyl-2-(((2-(trimethylammonium)ethyl)methyl)amino)naphthalene chloride (Patman), 6-dodecanoyl-2-dimethylaminonaphthalene (Laurdan), and 6-propionyl-2-dimethylaminonaphthalene (Prodan), were purchased from Molecular Probes (Eugene, OR). The spin-labeled quenchers 2-(3-carboxypropyl)-4,4-dimethyl-2-tridecyl-3-oxazolidinyloxy (5-doxyl-stearic acid) and 2-(14-carboxytetradecyl)-2-ethyl-4,4-dimethyl-3-oxazolidinyloxy (16-doxyl-stearic acid) were obtained from Aldrich (Steinheim, Germany). Acrylamide and HEPES were ordered from Fluka (Buchs, Switzerland). Solvents of spectroscopic grade were supplied by Merck (Darmstadt, Germany).

Preparation of Lipid Bilayers. The required volumes of chloroform solutions of DOPC (gel-to-liquid-crystalline phase transition: −18.3 °C[53]) and DOTAP (gel-to-liquid-crystalline phase transition: −11.9 °C[54]) were mixed in a glass tube with selected fluorescent dye (1 mol % of the final dye concentration). Solvents were evaporated under a stream of nitrogen while being continuously heated. The dry lipid film was then suspended in a 10 mM HEPES buffer (pH = 7.4, 100 mM NaCl) and vortexed for 4 min. Samples for the parallax measurements were prepared by mixing an appropriate spin-labeled compound with the lipid solution before evaporation, obtaining 15 mol % of final concentration of quencher. Large unilamellar vesicles (LUVs) were formed by extrusion through a polycarbonate membrane (Avestin, Ottawa, Canada) with 100 nm pores.[55] The prepared samples were transferred to a 1 cm quartz cuvette and equilibrated at the desired temperature for 10 min before each measurement. The final concentration of phospholipids in the cuvette was 1 mM, except for parallax measurements and quenching with acrylamide, where it was 0.2 and 0.08 mM, respectively.

Steady-State Fluorescence Measurements. All steady-state excitation and emission spectra acquisition were performed on a Fluorolog-3 spectrofluorometer (model FL3-11; Jobin Yvon Inc., Edison, NJ) equipped with a Xenon-arc lamp. The spectra were collected in 1 nm steps (2 nm bandwidths were chosen for both the

(19) Leidy, C.; Wolkers, W. F.; Jorgensen, K.; Mouritsen, O. G.; Crowe, J. H. *Biophys. J.* **2001**, *80*, 1819−1828.
(20) Shaikh, S. R.; Dumaual, A. C.; Jenski, L. J.; Stillwell, W. *Biochim. Biophys. Acta* **2001**, *1512*, 317−328.
(21) Xu, X.; London, E. *Biochemistry* **2000**, *39*, 843−849.
(22) Edidin, M. *Curr. Opin. Struct. Biol.* **1997**, *7*, 528−532.
(23) Brown, D. A.; London, E. *J. Membr. Biol.* **1998**, *164*, 103−114.
(24) Simons, K.; Ikonen, E. *Nature* **1997**, *387*, 569−572.
(25) Dietrich, C.; Bagatolli, L. A.; Volovyk, Z. N.; Thompson, N. L.; Levi, M.; Jacobson, K.; Gratton, E. *Biophys. J.* **2001**, *80*, 1417−1428.
(26) Epand, R. F.; Kraayenhof, R.; Sterk, G. J.; Sang, H. W. W. F.; Epand, R. M. *Biochim. Biophys. Acta* **1996**, *1284*, 191−195.
(27) Kaiser, R. D.; London, E. *Biochemistry* **1998**, *37*, 8180−8190.
(28) Sprong, H.; van-der-Sluijs, P.; van-Meer, G. *Nat. Rev.* **2001**, *2*, 504−513.
(29) Ikonen, E.; Simons, K. *Cell. Dev. Biol.* **1998**, *9*, 503−509.
(30) Killian, J. A.; von-Heijne, G. *TIBS* **2000**, *25*, 429−434.
(31) Ladokhin, A. S.; Isas, J. M.; Haigler, H. T.; White, S. H. *Biochemistry* **2002**, *41*, 13617−13626.
(32) White, S. H.; Wiener, M. C. In *Permeability and stability of lipid bilayers;* Disalvo, E. A., Simon, S. A., Eds.; CRC Press: Boca Raton, 1995; p 1.
(33) Marrink, S. J.; Mark, A. E. *J. Phys. Chem. B* **2001**, *105*, 6122−6127.
(34) Marrink, S. J.; Tieleman, D. P.; Buuren, A. R. V.; Berendsen, H. J. C. *Faraday Discuss.* **1996**, *103*, 191−201.
(35) Eastman, S. J.; Siegel, C.; Tousignant, J.; Smith, A. E.; Cheng, S. H.; Scheule, R. K. *Biochim. Biophys. Acta* **1997**, *1325*, 41−62.
(36) Langner, M. *Cell. Mol. Biol. Lett.* **2000**, *5*, 295−313.
(37) Gabrielska, J.; Przestalski, S.; Miszta, A.; Soczynska-Kordala, M.; Langner, M. *Appl. Organomet. Chem.* **2004**, *18*, 9−14.
(38) Langner, M.; Kleszczynska, H. *Cell. Mol. Biol. Lett.* **1997**, *2*, 15−24.
(39) Chattopadhyay, A.; London, E. *Biochemistry* **1987**, *26*, 39−45.
(40) Abrams, F. S.; London, E. *Biochemistry* **1993**, *32*, 10826−10831.
(41) Klymchenko, A. S.; Duportail, G.; Ozturk, T.; Pivovarenko, V. G.; Mely, Y.; Demchenko, A. P. *Chem. Biol.* **2002**, *9*, 1199−1208.
(42) Finer, E. G.; Darke, A. *Chem. Phys. Lipids* **1974**, *12*, 1−16.
(43) Westlund, P. O. *J. Phys. Chem. B* **2000**, *104*, 6059−6064.
(44) Mazeres, S.; Schram, V.; Tocanne, J. F.; Lopez, A. *Biophys. J.* **1996**, *71*, 327−335.
(45) Bernik, D. L.; Zubiri, D.; Tymczyszyn, E.; Disalvo, E. A. *Langmuir* **2001**, *17*, 6438−6442.
(46) Rheinstadter, M. C.; Ollinger, C.; Fragneto, G.; Demmel, F.; Salditt, T. *Phys. Rev. Lett.* **2004**, *93*, 108107.
(47) Tristram-Nagle, S.; Nagle, J. F. *Chem. Phys. Lipids* **2004**, *127*, 3−14.
(48) Hutterer, R.; Parusel, A. B. J.; Hof, M. *J. Fluoresc.* **1998**, *8*, 389−393.
(49) Hutterer, R.; Schneider, F. W.; Sprinz, H.; Hof, M. *Biophys. Chem.* **1996**, *61*, 151−160.
(50) Sykora, J.; Hof, M. *Cell. Mol. Biol. Lett.* **2002**, *7*, 259−261.
(51) Gurtovenko, A. A.; Patra, M.; Karttunen, M.; Vattulainen, I. *Biophys. J.* **2004**, *86*, 3461−3472.
(52) Silvius, J. R. *Biochim. Biophys. Acta* **1991**, *1070*, 51−59.
(53) Koynova, R.; Caffrey, M. *Biochim. Biophys. Acta −Rev. Biomembr.* **1998**, *1376*, 91−145.
(54) Hirsch-Lemer, D.; Barenholz, Y. *Biochim. Biophys. Acta −Biomembranes* **1998**, *1370*, 17−30.
(55) Hope, M. J.; Bally, M. B.; Mayer, L. D.; Janoff, A. S.; Cullis, P. R. *Chem. Phys. Lipids* **1986**, *40*, 89−107.

excitation and emission monochromators). The temperature in the cuvette holder was maintained within ±0.1 °C using a water-circulating bath. Red-edge excitation shifts (REES) were determined by detecting the fluorescence maxima when shifting the excitation wavelength toward the red edge of the absorption band.[56−59]

Fluorescence Quenching with Acrylamide. Acrylamide quenching experiments were carried out by measuring fluorescence intensity after sequentially adding small amounts of a stock solution of 5 M acrylamide in water to a stirred sample. The excitation wavelength used was 373 nm, and emission was monitored at the maximum of the emission spectrum. Quenching data were analyzed using the Stern−Volmer equation[60]

$$\frac{F_0}{F} = 1 + K_D[Q] \tag{1}$$

where F_0 and F are the fluorescence intensities in the absence and presence of the quencher, respectively, K_D is the Stern−Volmer quenching constant, and $[Q]$ is the concentration of the quencher in the sample.

Parallax Fluorescence Quenching. Parallax analysis of fluorescence quenching was used to determine the positions of the fluorescent probes within the membrane.[39,40] One mole percent of the dye was added to the lipid mixture with or without 15 mol % of one of the three free radical quenchers (TEMPO, 5-doxyl-stearic acid, 16-doxyl-stearic acid) present. The steady-state fluorescence intensity as well as fluorescence decays were measured at different emission wavelengths. Data collected for the three quenchers was analyzed in pairs to obtain the distance h of the dye from the bilayer center according to[40]

$$h = \frac{\pi C(h_{q1}^2 - h_{q2}^2) - \ln\left(\frac{F_1}{F_2}\right)}{2\pi C(h_{q1} - h_{q2})} \tag{2}$$

F is the fluorescence intensity in the presence of quencher, and h_q is the distance of the quencher from the bilayer center. The subscripts designate different quenchers, and C indicates the surface concentration of the quencher in molecules per unit area. The results obtained for different pairs of quenchers were collected and compared.

An alternative method, which was also used, is to calculate the distribution function of the quenched dye by fitting the collected data for all three quenchers with the parallax profile

$$\ln\left(\frac{F_0}{F(h_q)}\right) = \begin{bmatrix} \pi C[R_c^2 - (h_q - h)^2] & h_q - h < R_c \\ 0 & h_q - h \geq R_c \end{bmatrix} \tag{3}$$

where F_0 is the fluorescence intensity in the absence and $F(h_q)$ in the presence of the quencher located at a distance h_q from the bilayer center, and R_c is the radius of quenching.[61]

Time-Resolved Fluorescence Measurements. Fluorescence decays were recorded on a 5000U Single Photon Counting setup (IBH, Glasgow, U.K.) using an IBH laser diode NanoLED 11 (370 nm peak wavelength, 80 ps pulse width, 1 MHz maximum repetition rate) and a cooled Hamamatsu R3809U-50 microchannel plate photomultiplier. Emission decays were recorded at a series of wavelengths spanning the steady-state emission spectrum (400−540 nm) in 10 nm steps (emission slits: 8 nm bandwidths) at magic angle polarization. Additionally, a 399 nm cutoff filter was used to eliminate scattered light. The signal was kept below 2% of the light source repetition rate (1 MHz). Data were collected in 8192 channels (0.014 ns per channel) till the peak value reached 5000 counts. The time resolution, calculated as one-fifth of the full width at half-maximum (fwhm) of the instrument's response function, was about 16 ps. Fluorescence decays were fitted to multiexponential functions (two or three exponential components were used) using the iterative reconvolution procedure with IBH DAS6 software.

Solvent Relaxation. The methodology used to study the relaxation of hydrated lipid bilayers has already been described in detail elsewhere.[48,50,62,63] In short, time-resolved emission spectra (TRES) were obtained by the spectral reconstruction method[64] and fitted by a log-normal function in order to determine the position of the spectra $\nu(t)$ (in terms of their maxima) and their full widths at half-maximum (fwhm). The spectral response function (or correlation function), defined as

$$C(t) = \frac{\nu(t) - \nu(\infty)}{\nu(0) - \nu(\infty)} = \frac{\nu(t) - \nu(\infty)}{\Delta\nu} \tag{4}$$

was calculated by taking the estimated time-zero spectrum as $\nu(0)$. The so-called time-zero spectrum is the hypothetical fluorescence emission spectrum of the dye, which has vibrationally relaxed before any solvent motions. As shown, this spectrum cannot be measured directly in most systems due to the finite temporal resolution of the apparatus but can be estimated with absorption and steady-state emission spectra measured in a nonpolar solvent as described previously.[65] Comparison of the positions of time-zero spectra (the estimated and reconstructed one) also allows the percentage of the solvation process below the time resolution of the experimental setup to be determined.[66,67] To quantitatively characterize the solvent relaxation process, two parameters are determined. The first one, $\Delta\nu$, represents the overall emission shift. It has been shown that this parameter is proportional to the polarity of the dye environment.[64] In a phospholipid/water system, polarity is mainly attributed to water molecules; therefore, $\Delta\nu$ reflects the extent of lipid bilayer hydration. The absolute uncertainty of this parameter exceeds 200 cm^{-1} due to the uncertainty of the estimated time-zero spectrum. For Prodan, Laurdan, and Patman, which share the same fluorophore and time-zero spectra, we assumed the uncertainty to be 50 cm^{-1} for comparing the $\Delta\nu$ values within this study.

The second parameter assigned to a relaxation process is the relaxation time, which describes the mobility of the solvent molecules and is interpreted as a measure of the viscosity for neat solvents.[64] In the phospholipid bilayer at the level of glycerol, however, water hydrating the membrane is fully bound to the phospholipid molecules. Therefore, the slow relaxation kinetics observed in membranes is attributed to the collective relaxation of the dye environment and reflects membrane dynamics rather than the motions of water molecules.[66,67] The mean solvent relaxation time was calculated according to the following formula

$$\tau_r \equiv \int_0^\infty C(t)\, dt \tag{5}$$

Compared to fitting the relaxation function by kinetic models,[66,68] such an approach does not require any knowledge about the solvation process a priori.[64] The intrinsic uncertainty for this parameter was assumed to be ∼20 ps based on the time resolution of the experimental setup.

The temporal behavior of the fwhm of the TRES provides useful information on the extent of the observed solvent relaxation. The

(56) Chattopadhyay, A.; Mukherjee, S. *Langmuir* **1999**, *15*, 2142−2148.
(57) Demchenko, A. P. *Biophys. Chem.* **1982**, *15*, 101−109.
(58) Lakowicz, J. R.; Keatingnakamoto, S. *Biochemistry* **1984**, *23*, 3013−3021.
(59) Satoh, T.; Okuno, H.; Tominaga, K.; Bhattacharyya, K. *Chem. Lett.* **2004**, *33*, 1090−1091.
(60) Lakowicz, J. R. *Principles of Fluorescence Spectroscopy*, 2nd ed.; Kluwer-Plenum Press: New York, 1999.
(61) Thoren, P. E. G.; Persson, D.; Esbjorner, E. K.; Goksor, M.; Lincoln, P.; Norden, B. *Biochemistry* **2004**, *43*, 3471−3489.
(62) Hof, M. In *Applied Fluorescence in Chemistry, Biology, and Medicine;* Rettig, W., Ed.; Springer-Verlag: Berlin, 1999; p 439.
(63) Jurkiewicz, P.; Sykora, J.; Olzynska, A.; Humplickova, J.; Hof, M. *J. Fluoresc.* **2005**, *15*, 883−894.
(64) Horng, M. L.; Gardecki, J. A.; Papazyan, A.; Maroncelli, M. *J. Phys. Chem.* **1995**, *99*, 17311−17337.
(65) Fee, R. S.; Maroncelli, M. *Chem. Phys.* **1994**, *183*, 235−247.
(66) Sykora, J.; Kapusta, P.; Fidler, V.; Hof, M. *Langmuir* **2002**, *18*, 571−574.
(67) Nilsson, L.; Halle, B. *Proc. Natl. Acad. Sci. U.S.A.* **2005**, *102*, 13867−13872.
(68) Sykora, J.; Jurkiewicz, P.; Epand, R. M.; Kraayenhof, R.; Langner, M.; Hof, M. *Chem. Phys. Lipids* **2005**, *135*, 213−221.

experiments carried out in phospholipid bilayers[62,69] and also in the supercooled liquids[70] have shown that the fwhm passes a maximum during the solvation process. This is in a good agreement with the idea of a nonuniform spatial distribution of solvent response times.[70,71] It has been shown that in homogeneous systems of low molar mass molecules, the fwhm decays monotonically. In spatially inhomogeneous systems, however (i.e., where the microenviroments of the fluorophores differ), the relaxation behavior is different since the solvent shells of individual fluorophores distributed in the system respond with different rates to changes in the local electric field (which also spatially varies). This gives rise to a new phenomenon, which reflects the time distribution of phases of relaxations of individual solvation shells during the relaxation. The overall transient inhomogeneity increases significantly during the solvation and then decreases once the solvation finishes and the equilibrated excited state is reached. That is why the fwhm of TRES, which gives the measure of inhomogeneity of dyes microenvironments, passes a pronounced maximum. This effect gives the origin for the method of checking whether the entire response or merely part of it was captured within the time window of the experiment. If only a decrease in the fwhm is observed, it means that the early part of the relaxation process is possibly beyond the time resolution of the equipment. In contrast, if only an increase is detected, the process is fairly slow under given conditions and the lifetime of the used fluorophore is not long enough to completely monitor the relaxation. It should be mentioned that in the case of Aerosol-OT reverse micelles it is suggested from experiment[72] and by computer simulations[73] that the time dependence of the fwhm is due to self-diffusion of the excited probe (4-(dicyanomethylene-2-methyl-6(*p*-dimethylaminostyryl)-4*H*-pyran) from nonpolar to polar location. However, since the chromophores of Laurdan and Patman are anchored in the hydrophobic part of the bilayer, this alternative explanation appears unlikely for our lipid experiments.

Dynamic Light Scattering. The size distribution of vesicles was measured using dynamic light scattering (DLS). The light scattering setup (ALV, Langen, Germany) consisted of a 633 nm He−Ne laser, ALV CGS/8F goniometer, ALV High QE APD detector, and ALV 5000/EPP multibit, multitau autocorrelator. Prior to measurement, samples were filtered through 0.45 μm Acrodisc filters. Experimental, normalized intensity autocorrelation functions were analyzed using cumulant analysis[74] and constrained regularized fitting based on the CONTIN method.[75] Mean vesicles sizes, along with the standard deviation, were calculated from surface-weighted size distributions.

Results and Discussion

Effect of Surface Charge on Vesicle Size Distribution. As we have recently shown, the curvature of a membrane can affect its hydration properties.[68] Since the surface charge of cationic vesicles may influence both their size and their surface properties, the morphology of liposomes should be well characterized after preparation. Dynamic light scattering was used for this purpose. Vesicle suspensions were measured at a right angle, and since fluorescence dyes are located on the sphere surface, size distributions were surface weighted. In addition, the radius of gyration was calculated based on light scattering measurements at different angles. When the hydrodynamic radii were compared with the gyration radii, no significant discrepancy was observed for any of the samples used. This justifies the hard-sphere model used for fitting the distributions. In addition, vesicle size distributions measured shortly after sample preparation and 5 days later do not show any relevant differences, providing evidence for liposomes stability. The mean radius for all the formulations used was 40 ± 5 nm. All distributions were unimodal with a standard deviation smaller than 15 nm. Taking into account the fact that the mean relaxation times measured by Patman for vesicles with a radius of 10 and 100 nm differ by only ~25%,[68] we can safely assume that curvature effects can be neglected.

Determining the Fluorophore Location within the Lipid Bilayer. Solvent relaxation in the lipid membranes is 4 orders of magnitude slower than in the bulk—the meantime constant in pure water is 0.3 ps,[76] whereas at the glycerol level of a fully hydrated phospholipid bilayer in the liquid crystalline state it is about 2 ns.[66] Such a large change in this parameter on a distance of only 1 nm results in enormous gradients of solvation properties along the membrane normal. This substantiates the need for precisely knowing the location of a polarity-sensitive fluorescence dye, which allows the relaxation properties to be well characterized. To achieve this, the parallax method was used as described elsewhere.[39,77] Some indications regarding the locations of Prodan, Laurdan, and Patman within the membrane can be found in the literature, but systematic experimental studies are still lacking. All three dyes have the same fluorophore, which consists of an electron-donating dimethylamino group and an electron-withdrawing carbonyl group of a different fatty acid residue, separated by a naphthalene ring. The naphthalene ring ensures a substantial increase of dipole moment upon electronic excitation.

Prodan, synthesized by Weber and Farris,[78] contains a short propionyl group, which is believed to be positioned in the outermost region of the interface.[79] This results in a poorly defined location, and consequently, any measurements performed with Prodan should be evaluated with great care (see, ref 80 for example). We have shown that analysis of the TRES shape gives an unambiguous indication of whether the solvent relaxation approach is appropriate for a specific system. If other processes, besides solvation, take place or if more than one homogeneous population of the dye is present, the fwhm profile clearly differs from the one normally observed.[50,66,80]

Laurdan and Patman have the same fluorophore as Prodan but are modified so that their location within the membrane is more certain. Laurdan has a longer hydrocarbon chain (11 carbons) attached to the carbonyl group, which anchors the molecule in the hydrophobic part of the bilayer. It is commonly assumed that its fluorophore stays at the level of the glycerol backbone.[81] This assumption is a result of a comparison between its fluorescent properties under different experimental conditions.[81−83] With one exception,[84] however, no exact determinations of the location of Laurdan in the membranes have been performed.

Patman, in addition to a palmitoyl tail, possesses a trimethylammonium group, which orients the alkylamino end of the fluorophore toward the lipid−water interface[85] and stabilizes the dye position in the bilayer due to interactions with charged

(69) Sykora, J.; Mudogo, V.; Hutterer, R.; Nepras, M.; Vanerka, J.; Kapusta, P.; Fidler, V.; Hof, M. *Langmuir* **2002**, *18*, 9276−9282.
(70) Yang, M.; Richert, R. *J. Chem. Phys.* **2001**, *115*, 2676−2680.
(71) Richert, R. *J. Chem. Phys.* **2001**, *115*, 1429−1434.
(72) Dutta, P.; Sen, P.; Mukherjee, S.; Halder, A.; Bhattacharyya, K. *J. Phys. Chem. B* **2003**, *107*, 10815−10822.
(73) Faeder, J.; Ladanyi, B. M. *J. Phys. Chem. B* **2005**, *109*, 6732−6740.
(74) Koppel, D. E. *J. Chem. Phys.* **1972**, *57*, 4814-&.
(75) Provencher, S. W. *Comput. Phys. Commun.* **1982**, *27*, 213−227.
(76) Jimenez, R.; Fleming, G. R.; Kumar, P. V.; Maroncelli, M. *Nature* **1994**, *369*, 471−473.
(77) Klymchenko, A. S.; Duportail, G.; Demchenko, A. P.; Mely, Y. *Biophys. J.* **2004**, *86*, 2929−2941.
(78) Weber, G.; Farris, F. J. *Biochemistry* **1979**, *18*, 3075−3078.
(79) Chong, P. L. G. *Biochemistry* **1988**, *27*, 399−404.
(80) Hutterer, R.; Hof, M. *Z. Phys. Chem.−Int. J. Res. Phys. Chem. Chem. Phy.* **2002**, *216*, 333−346.
(81) Parasassi, T.; Krasnowska, E. K.; Bagatolli, L.; Gratton, E. *J. Fluoresc.* **1998**, *8*, 365−373.
(82) Chong, P. L. G.; Wong, P. T. T. *Biochim. Biophys. Acta* **1993**, *1149*, 260−266.
(83) Viard, M.; Gallay, J.; Vincent, M.; Paternostre, M. *Biophys. J.* **2001**, *80*, 347−359.
(84) Antollini, S. S.; Barrantes, F. J. *Biochemistry* **1998**, *37*, 16653−16662.
(85) Lakowicz, J. R.; Bevan, D. R.; Maliwal, B. P.; Cherek, H.; Balter, A. *Biochemistry* **1983**, *22*, 5714−5722.

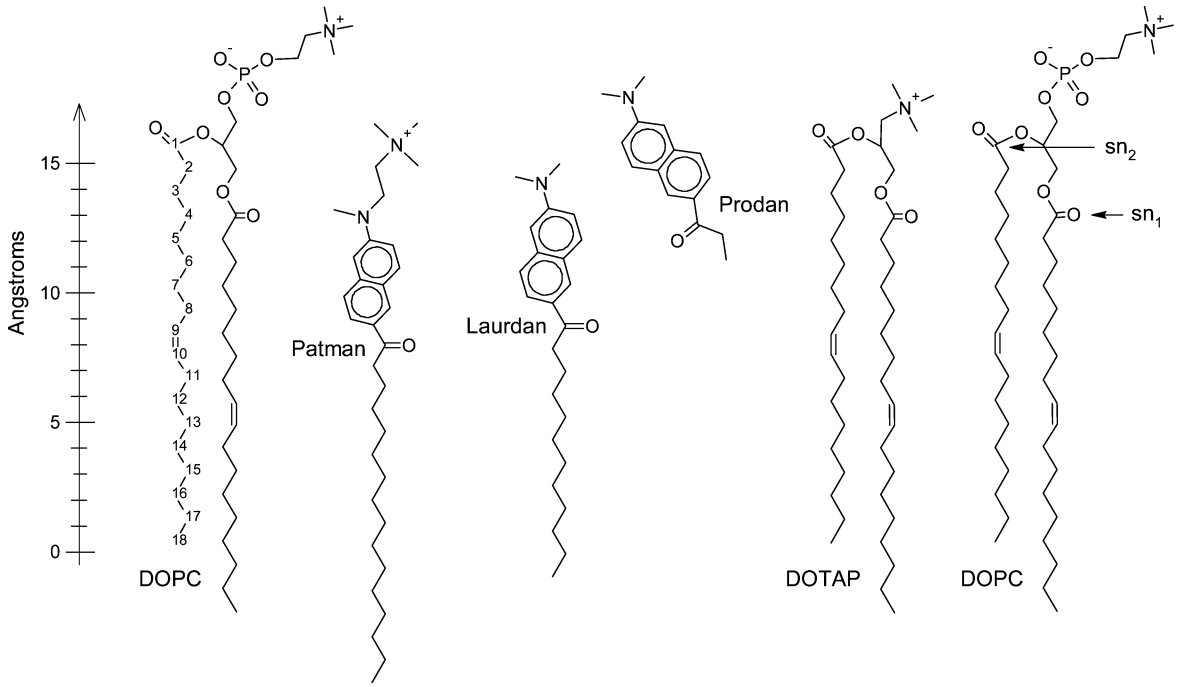

Figure 1. Schematic diagram of the location of Patman, Laurdan, and Prodan in a membrane composed of dioleoylphosphatidylcholine (DOPC) and dioleoyltrimethylammoniumpropane (DOTAP). The positions of sn_1 and sn_2 carbonyls are indicated by arrows. The carbon atoms of the sn_2 chain are numbered. The scale on the left shows the approximate distance from the bilayer center. Upon addition of DOTAP, the position of Patman changes and differs from the one shown here. See text for details on the dye locations.

phospholipid headgroups. Our previous studies have shown that the position of Patman does not change and that a single dye population is always present. NMR studies have shown that Patman is embedded deeper in the bilayer compared to Prodan and that its movement is more restricted.[49]

Application of parallax quenching allowed us to determine the distance of the fluorophores of Laurdan and Patman from the bilayer center. This distance, calculated using eq 2, was about 11.4 Å for Laurdan, regardless of the selected pair of quenchers. The obtained value is in good agreement with the position of the probe (~9.8 Å) measured in the cell membrane of *Torpedo marmorata* enriched with nicotine acetylcholine receptors.[84] The radius of the sphere of quenching, calculated according to eq 3, was equal to 12.8 Å, again in good agreement with values reported elsewhere.[40] This value was used to determine the position of Patman with eq 2, resulting in a distance of 10.4 Å from the bilayer center. The results obtained for Prodan were not consistent, suggesting a broad distribution of this dye, and are therefore not presented here. The statistical character of the location of both dyes and quenchers implies that all the obtained values are averages and that the actual values can fluctuate.[39] The determined position of the two dyes are indicated in the schematic lipid bilayer representation of Figure 1, together with the Prodan position found in the literature.[81]

The difference in localization between the chromophores of Patman and Laurdan is 1 Å, which is close to the uncertainty of the parallax method. However, the measurements were performed several times with exactly the same differences in positions of these two dyes. It is worth mentioning that this small 1 Å difference in position is occurring in the bilayer region where an enormous gradient of water concentration is present.[18] The mean solvent relaxation times are varying from the position of Patman (see Figure 1) to bulk water from about 2 ns[66,68] to hundreds of femtoseconds,[76] respectively. Considering these facts as well as the high sensitivity of the solvent relaxation technique, we believe that the 1 Å difference causes the differences in the mean solvent

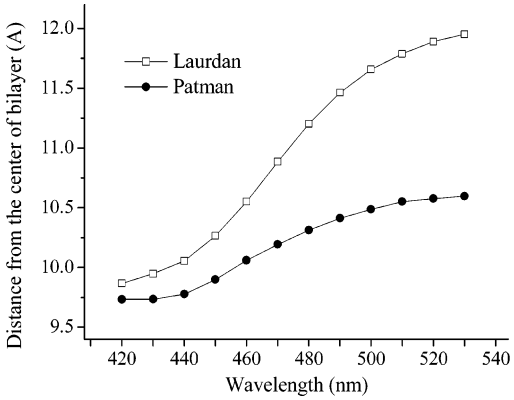

Figure 2. Wavelength-dependent position of Laurdan (open squares) and Patman (filled circles) in terms of distance from the center of bilayer, calculated according to eq 2 for different emission wavelengths. The dye was excited at 373 nm. The measurements were performed at 20 °C.

relaxation times (Figure 9) as well as in the corresponding $\Delta\nu$ values (Figure 8) reported in this manuscript.

The average positions of Laurdan and Patman presented above were determined for the emission maxima, i.e., 493 and 475 nm, respectively. The excitation wavelength was 373 nm. A strong dependence of quenching efficiency on the emission wavelength, however, was observed. The calculated distances of the dyes from the membrane center increase with wavelength (Figure 2).

In a steady-state experiment, an increase in the detection wavelength of the emission leads to photoselection of the chromophores, which are in a more relaxed and/or more polar environment, since solvent relaxation becomes faster and the amount of water increases when moving toward the lipid/water interface.[50] Thus, the wavelength dependence of the quenching rate can provide some information on the heterogeneity of the chromophore's location along the *z* axis. These two dyes are different in this respect, i.e., a stronger dependence of the calculated position on the emission wavelength is observed for

Table 1. Quenching of Patman and Laurdan Embedded in DOPC/DOTAP LUVs with Acrylamide

	Patman		Laurdan	
[DOTAP] (mol %)	K_D (M^{-1})[a]	R^2 [b]	K_D (M^{-1})[a]	R^2 [b]
0	0.274 ± 0.003	99.9	0.340 ± 0.005	99.9
30	0.314 ± 0.003	99.9	0.347 ± 0.004	99.9
50	0.317 ± 0.004	99.9	0.350 ± 0.006	99.9
100	0.314 ± 0.006	99.9	0.369 ± 0.003	99.9

[a] K_D =Stern−Volmer constants as defined by eq 1 and calculated by fitting the data points to a straight line. [b] R^2 =square of the correlation coefficient of fitting in percents.

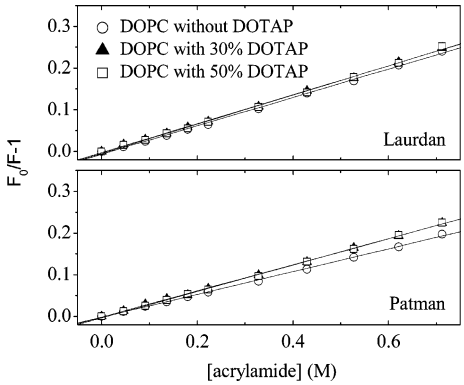

Figure 3. Acrylamide quenching of Patman and Laurdan embedded in LUVs consisting of DOPC (open circles), DOTAP/DOPC (3:7) (filled triangles), and DOTAP/DOPC (1:1) (open squares). Acrylamide was added to a stirred cuvette from a 5 M stock solution. Measurements were performed at room temperature, and excitation wavelength was 373 nm.

Laurdan (~2 Å) than for Patman (<1 Å). This can be attributed to the lack of the trimethylammonium group and a shorter hydrophobic chain of Laurdan. The conclusion that the location of the chromophores shows a certain distribution along the *z* axis might be supported by the determined (identical within the experimental error) REES shifts for Laurdan and Patman of 6 ± 1 and 4 ± 1 nm at 10 and 20 °C, respectively. It is worth mentioning that in a recent work the red-edge effect was combined with the solvent relaxation approach in lipid vesicles.[86] It was shown that even using a dye (coumarin 480) with a rather undefined location, tuning of the excitation wavelength allows studying the solvation dynamics of certain domains of the bilayer/water system.

Acrylamide Quenching. The presence of positively charged DOTAP may bias parallax quenching analysis due to electrostatic interactions between cationic lipid molecules and the carboxyl groups of DOXYL quenchers. That is why quenching with a neutral compound—acrylamide—was performed in order to determine the effect of DOTAP on the dye position. Water-soluble acrylamide is commonly used to determine the depth of membrane penetration by proteins and other fluorescent compounds.[60] In our work, acrylamide quenching was used to study the effect of surface cationic charge on the accessibility of fluorescence probes from the bulk phase. It was assumed that changes of the quenching constant as a function of DOTAP concentration can be correlated to the different locations of the dye, an increase in the quenching constant indicating increased dye accessibility from water. The obtained Stern−Volmer constants for Patman and Laurdan are listed in Table 1. Examples of original quenching data are presented in Figure 3. The quenching plots for Patman and Laurdan were linear. The quenching plots for Prodan, on the other hand, were not perfectly linear (data not shown), which is again an indication for a rather heterogeneous localization of Prodan within the bilayer.[79,87]

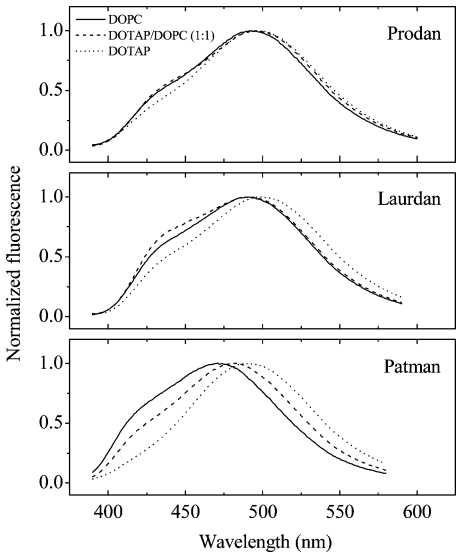

Figure 4. Steady-state emission spectra of Prodan, Laurdan, and Patman collected for LUVs formed from DOPC (solid line), DOPC/DOTAP (1:1) (dashed line), and DOTAP (dotted line) at 10 °C. The excitation wavelength was 373 nm.

An interesting result is the relocation of Patman, which moves out of the bilayer when the content of DOTAP changes from 0 to 30 mol %. Further addition of DOTAP does not change the position of Patman any further. In the case of Laurdan, we observe only a small increase of the quenching constant, which means there is no significant change in its position. The increased accessibility of the fluorophore to acrylamide may also be explained by the elevated penetration of the quencher into the interfacial region of the lipid bilayer. We excluded such a possibility based on our SR results (see the solvent relaxation section later in the text), which indicate that the membrane becomes tighter when the amount of DOTAP rises to 30 mol %. Consequently, the observed rise in the quenching efficiency for Patman is a consequence of its relocation. When the amount of DOTAP in the membrane exceeds 30 mol %, the lipid bilayer relaxes gradually, which does not affect the quenching constant of Patman. The increase in the quenching efficiency for Laurdan when the amount of DOTAP changes from 50 to 100 mol % can be interpreted as elevated membrane penetration by the quencher or the altered position of the probe.

Steady-State Fluorescence Spectra. Excitation and emission spectra of Prodan, Laurdan, and Patman incorporated into LUVs were determined. Representative normalized emission spectra of the three dyes for 0, 50, and 100 mol % of DOTAP in DOPC at 10 °C are shown in Figure 4.

The largest changes were observed for Patman, namely, a red shift occurs and the shoulder on the blue side of the spectrum disappears with increasing DOTAP fraction. Moreover, the red-edge excitation shift is decreasing from 6 ± 1 to 4 ± 1 nm at 10 °C when increasing the DOTAP content in liposome membrane from 0 to 50 mol %. These observations may be interpreted in terms of a DOTAP-induced relocalization of Patman toward a more polar and/or less viscous microenvironment. The changes in the steady-state spectra are less pronounced for Laurdan, whose emission spectrum for liposomes containing 50 mol % of DOTAP is the least red-shifted one. The spectra of Prodan are not modified

(86) Sen, P.; Satoh, T.; Bhattacharyya, K.; Tominaga, K. *Chem. Phys. Lett.* **2005**, *411*, 339−344.

(87) Geddes, C. D. *Meas. Sci. Technol.* **2001**, *12*, R53−R88.

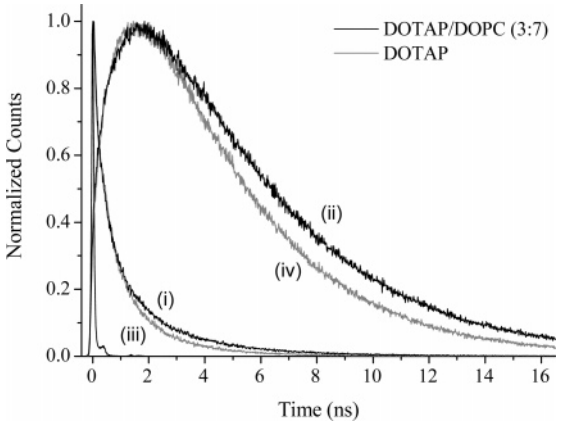

Figure 5. Fluorescence decays of Laurdan (λ_{ex} = 373 nm) at 10 °C for 30 mol % of DOTAP in DOPC (black lines) at 400 (i) and 540 nm (ii) and pure DOTAP (grey lines) at 400 (iii) and 540 nm (iv).

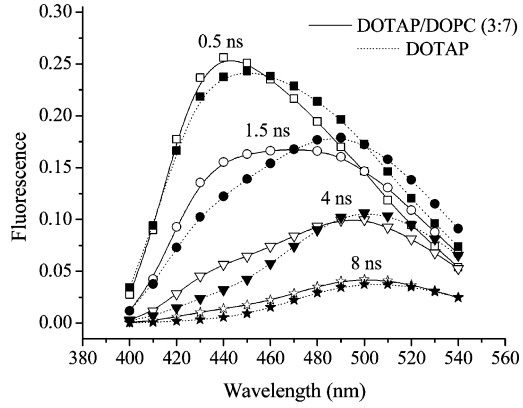

Figure 6. Reconstructed time-resolved emission spectra (TRES) for Laurdan at 10 °C for 30 mol % of DOTAP in DOPC (empty symbols and solid lines) and pure DOTAP (filled symbols and dotted lines) at 0.5 (squares), 1.5 (circles), 4 (triangles), and 8 ns (stars) after excitation. For details about the reconstruction procedure, see the Materials and Methods section.

by the presence of DOTAP, except for a minute red shift for liposomes formed from DOTAP alone. It is worth noting that the spectra of Patman are narrower and less red-shifted than the spectra of the two other dyes. This may indicate that the dye is in a less polar (or more restricted) environment. Such a conclusion is not straightforward, however, since steady-state spectra depend on viscosity as well. To weigh the effect of the two processes, analysis of time-resolved emission spectra is required.

Time-Resolved Emission Spectra (TRES) and SR Analysis. Laurdan measurements are used in this study to illustrate the typical shape of recorded fluorescence decays as well as reconstructed TRES and demonstrate data analysis that results in the parameters discussed later. In Figure 5 fluorescence decays of Laurdan for 30 and 100 mol % of DOTAP in DOPC at 400 and 540 nm, respectively, are presented. Figure 6 shows the reconstructed TRES for Laurdan in lipid mixtures mentioned above collected at 0.5, 1.5, 4, and 8 ns after excitation.

The gradual shift to longer wavelengths and a decrease of the intensity maxima are clearly visible. The spectra became wider with time after excitation. The spectral difference between the two samples persists up to the 8th ns, when the spectra superimpose. For liposomes formed from pure DOTAP, the spectral shift toward longer wavelengths occurs faster.

The TRES of all samples were analyzed in terms of their positions and widths. Figure 7 shows the positions of spectra

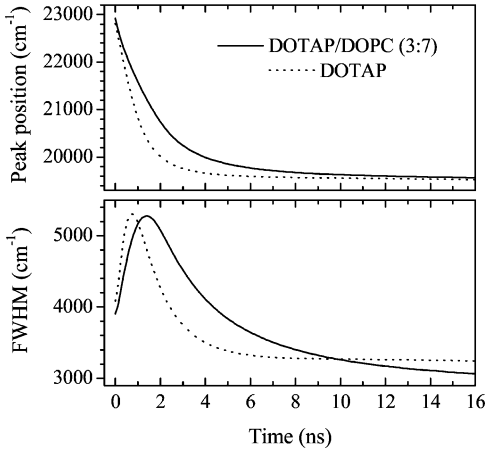

Figure 7. Position of the maximum and full width at half-maximum (fwhm) of TRES obtained for Laurdan at 10 °C for 30 mol % of DOTAP in DOPC (solid lines) and pure DOTAP (dotted lines) as a function of time after excitation.

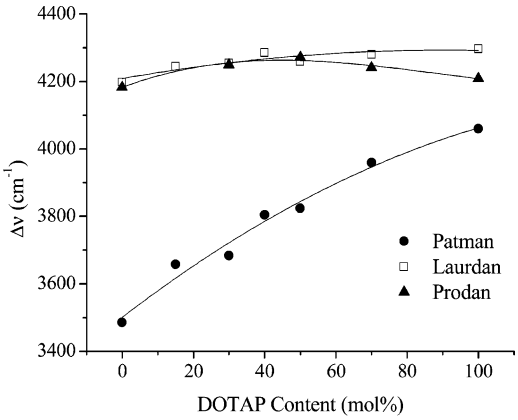

Figure 8. Solvent relaxation $\Delta\nu$ parameter for Prodan (filled triangles), Laurdan (open squares), and Patman (filled circles) in DOPC/DOTAP LUVs as a function of DOTAP content. Measurements were performed at 10 °C. The solid lines are polynomial fits and shown only as a guide to the eye.

maxima and widths at half-maximum as a function of time for two selected lipid mixtures (30 and 100 mol % of DOTAP).

The shift in the emission maximum for Laurdan incorporated into a lipid bilayer formed from pure DOTAP is not only faster but also larger. This is due to the infinite time it takes the curve to converge to smaller wavenumbers, i.e., $\nu_{100\%\ DOTAP}(\infty) < \nu_{30\%\ DOTAP}(\infty) \rightarrow \Delta\nu_{100\%\ DOTAP} > \Delta\nu_{30\%\ DOTAP}$. The Laurdan fwhm profile for liposomes formed from pure DOTAP is shifted to shorter times and larger wavenumbers, which indicates that the environment of Laurdan is more mobile and more heterogeneous, respectively.

The fwhm profiles for all three dyes (Patman, Laurdan, Prodan) in all investigated lipid systems show clear maxima, providing evidence that solvent relaxation takes place within the time scale of the experiment and suggesting a unimodal distribution of the chromophores. The $\nu(0)$ for the dyes used here in DOPC LUVs was found to be 23 800 cm^{-1} and not affected by the presence of DOTAP.

Effect of DOTAP on Membrane Hydration and Mobility. Total emission shift ($\Delta\nu$), as a function of DOTAP concentration in DOPC membranes, is presented in Figure 8.

The effect of DOTAP on $\Delta\nu$ for Laurdan and Prodan was within the uncertainty of the method (50 cm^{-1}). Completely different results were registered for Patman, for which a steep increase of $\Delta\nu$ with increasing DOTAP content is observed.

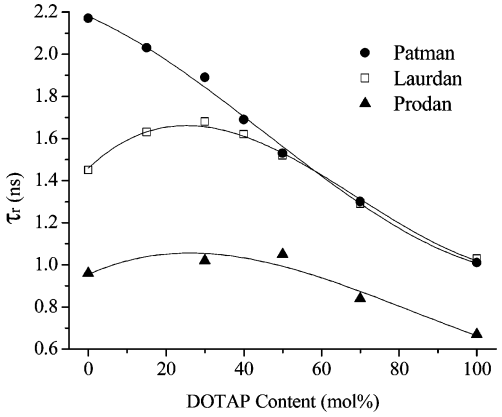

Figure 9. Mean solvent relaxation time τ_r (defined by eq 5) for Prodan (filled triangles), Laurdan (open squares), and Patman (filled circles) in DOPC/DOTAP LUVs as a function of DOTAP content. Measurements were performed at 10 °C. The solid lines are best polynomial fits and shown only as a guide to the eye.

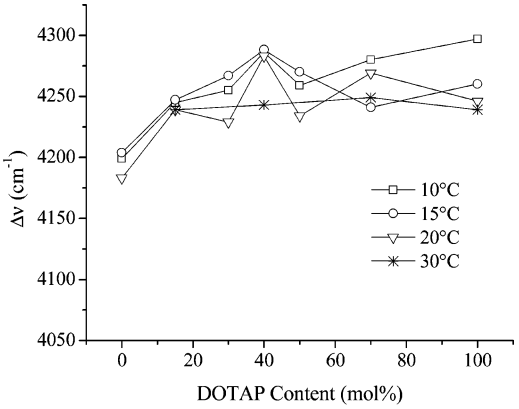

Figure 10. Solvent relaxation $\Delta\nu$ parameter for Laurdan in DOPC/DOTAP LUVs as a function of DOTAP content. Samples were measured at 10 (squares), 15 (circles), 20 (triangles), and 30 °C (asterisks).

These changes are larger than any previously observed for liquid crystalline membranes. To interpret them correctly, precise determination of Patman position was found to be crucial. This position changes when the fraction of DOTAP increases from 0 to 30 mol % (Table 1). Thus, the rise in $\Delta\nu$ in this range of DOTAP content cannot be interpreted as elevated membrane hydration. When the fraction of DOTAP is larger than 30 mol %, however, the location of Patman does not change (Table 1) and the continuous increase of $\Delta\nu$ can be interpreted as an increase in polarity in the vicinity of the probe. In summary, when the fraction of DOTAP in a DOPC membrane exceeds 30 mol %, membrane hydration increases at the level of Patman (i.e., water penetrates deeper into the membrane), while at the level of Laurdan and Prodan it does not. Apparently, Laurdan and Prodan are located in a membrane region where hydration is so extensive that any modification of the lipid bilayer composition, resulting in an increase of hydration, has little effect. From the $\Delta\nu$ data it can be concluded that for DOTAP content ranging between 30 and 100 mol % hydration of the DOPC/DOTAP membrane increases, whereas at lower DOTAP contents no changes in membrane hydration are detectable.

Integrated solvent relaxation time (eq 5) was a good indicator of determined solvent relaxation kinetics, as the spectral response functions did not vary in shape. The dependences of relaxation time determined for the three dyes as a function of the amount of DOTAP in the lipid bilayer are presented in Figure 9. Pronounced maxima at around 30 mol % of DOTAP are reported by Laurdan and Prodan (the different behavior of Patman is attributed to its relocation).

The kinetics of dielectric relaxation in the lipid membrane is often interpreted as the freedom of movement of water hydrating the membrane. At the level where the used dyes were located, however, water molecules are believed to be fully bound to membrane phospholipids. Therefore, the dynamics of the system as a whole should be considered[67] rather than the slow dynamics of individual water molecules, as previously postulated for subnanosecond dynamics observed for protein surfaces.[88,89] We discuss the results in a general way, referring to bilayer mobility and rigidity in terms of lipid packing.[49]

The relaxation time constant depends nonmonotonically on the concentration of DOTAP. Addition of up to 30 mol % of cationic lipid to the lipid bilayer increases the rigidity of the corresponding hydrated functional groups in the vicinity of the chromophore (see Figure 1), which is reflected by an elevated integrated relaxation time. Further increase of the amount of cationic lipid loosens the lipid bilayer interface, which is indicated by a decrease of the relaxation time. This result is an experimental confirmation of the molecular dynamics simulations performed by Gurtovenko et al.[51] Their work shows that membrane lipid headgroups in the liquid crystalline state can rearrange upon interacting with charged residues within the membrane interface, as postulated previously.[90] Namely, the P−N dipoles of phosphatidylcholine were found to change their orientation from ∼10° to the membrane surface to around 60° in the presence of DMTAP. This effect explains the results presented in Figure 9. At low DOTAP concentrations, the electrostatic repulsion between cationic TAP groups and the N^+ of the choline moiety causes reorientation of PC headgroups to a more vertical position. At the same time, cationic TAP attracts the P^- of PC. Both effects result in membrane compression. At larger DOTAP concentrations, the cationic charges repel, resulting in bilayer expansion. It has been shown elsewhere that when the extent of such an expansion is large enough, a transition to the interdigitated phase is possible.[91] Our results also qualitatively agree with the theoretical studies of Levadny and Yamazaki, who assumed that PC dipoles are organized latterly around TAP clusters.[92] Their analysis predicts that there is a nonmonotonic dependence of membrane packing on the fraction of cationic lipid present in the lipid bilayer with a condensation maximum (minimum area per lipid) at 50 mol % of DMTAP mixed with DMPC. The discrepancy between our results and those from the literature may result from different acyl chain lengths (mirystoyl instead of oleoyl used in this work). Calorimetric studies on dipalmitoylphosphatidylcholine with dihexadecyldimethylammonium chloride, however, have shown that a maximum transition temperature occurs at ∼35 mol % of cationic compound,[52] which is in excellent agreement with our results.

Effect of Temperature on the SR of Laurdan. The effect of temperature on the SR parameters of Laurdan was measured for lipid bilayers formed from various mixtures of DOTAP and DOPC. The resulting curves of $\Delta\nu$ and τ_r for 10, 15, 20, and 30 °C are presented in Figures 10 and 11, respectively. The data show that temperature does not alter the level of hydration, but

(88) Bhattacharyya, K.; Bagchi, B. *J. Phys. Chem. A* **2000**, *104*, 10603−10613.
(89) Pal, S. K.; Zewail, A. H. *Chem. Rev.* **2004**, *104*, 2099−2123.
(90) Scherer, P. G.; Seelig, J. *Biochemistry* **1989**, *28*, 7720−7728.
(91) Ryhanen, S. J.; Alakoskela, J. M. I.; Kinnunen, P. K. J. *Langmuir* **2005**, *21*, 5707−5715.
(92) Levadny, V.; Yamazaki, M. *Langmuir* **2005**, *21*, 5677−5680.

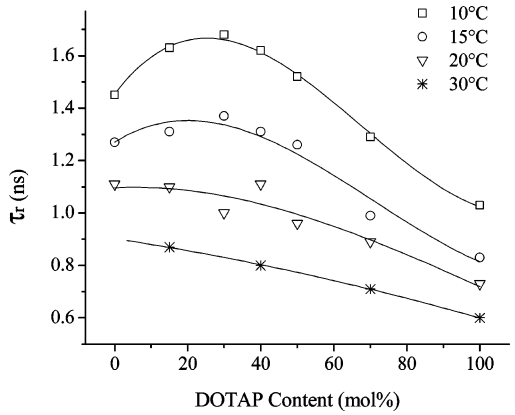

Figure 11. Mean relaxation time τ_r (eq 5) for Laurdan in DOPC/DOTAP LUVs as a function of DOTAP content. Measurements were performed at 10 (squares), 15 (circles), 20 (triangles), and 30 °C (asterisks). The solid lines are best polynomial fits and shown only as a guide to the eye.

the kinetics of relaxation is strongly affected (the higher the temperature the faster the relaxation).

The temperature rise results in higher bilayer mobility and a reduction of the maximum, which is most evident at 10 °C, which gradually diminishes at higher temperatures and disappears completely at 30 °C (Figure 11). Electrostatic effects are hindered by the elevated Brownian motions of all the elements of the system at higher temperatures. As expected, this eliminates the compression effect for membranes formed from 0 to 30 mol % of DOTAP, whereas for higher DOTAP concentrations lateral repulsion is still present.

Conclusions

Solvent relaxation based on time-resolved measurements of fluorescent probes with defined locations within the lipid bilayer is a valuable and unique tool, suitable for monitoring the hydration and organization of fully hydrated biological and model membranes. The SR properties of DOPC/DOTAP cationic membranes as well as the locations of the fluorescent probes—Patman and Laurdan—were determined. Quenching with acrylamide provided a simple and reliable test for potential dye relocation, particularly important in studies of lipid membranes in which large gradients of hydration properties are present. Wavelength-dependent parallax quenching, in turn, is capable of precisely defining the probing depth of the bilayer. Using a set of dyes that share the same spectroscopic properties but differ in their location within the bilayer allows the obtained SR parameters to be compared at different levels inside the membrane. Synthesis of other such sets of probes is still needed.

The observed nonmonotonic dependence of relaxation properties on DOTAP content in the DOPC bilayer supports a scenario of headgroup rearrangement in mixtures of cationic and zwitterionic lipids.[51,90,91,93] This finding may have important implications for the development of synthetic genetic information carriers, e.g., it correlates with the interaction profile of cationic vesicles with oligonucleotides for which maximum association was found at ∼25% of DOTAP.[94]

Acknowledgment. The authors thank Magdalena Siwko and Guy Duportail for their valuable suggestions and Karel Procházka for access to dynamic light scattering instrumentation. Financial support by the Grant Agency of the Academy of Sciences of the Czech Republic (P. J. and A.O. via A400400503) and the Ministry of Education and Sport of the Czech Republic (M.H. via LC06063) is gratefully acknowledged.

LA061597K

(93) Zhang, L. F.; Spurlin, T. A.; Gewirth, A. A.; Granick, S. *J. Phys. Chem. B* **2006**, *110*, 33−35.
(94) Jurkiewicz, P.; Okruszek, A.; Hof, M.; Langner, M. *Cell. Mol. Biol. Lett.* **2003**, *8*, 77−84.